

## SYNTHESIS AND STRUCTURAL STUDIES OF NICKEL SULPHIDE AND PALLADIUM SULPHIDE NANOCRYSTALS

P. A. AJIBADE\*, A. NQOMBOLO

*Department of Chemistry, University of Fort Hare, Private Bag X1314, Alice 5700, South Africa*

We report the synthesis of NiS and PdS nanoparticles using imidazolyl dithiocarbamate single source precursor's thermolysed in hexadecylamine. The nanocrystals were characterized with UV-Vis absorption and emission spectroscopy, X-ray diffraction, Transmission electron microscopy, scanning electron microscopy and energy dispersive X-ray spectroscopy. Absorption spectra of the NiS and PdS nanoparticles are blue shifted indicating they are quantum confined due to their small crystallite sizes while the photoluminescence spectra shows narrow emissions that are red-shifted. The XRD patterns of the NiS nanocrystals were indexed to rhombohedral crystalline phase while the XRD of the PdS revealed the tetragonal crystalline phase. The TEM analysis indicate that the individual NiS nanoparticles are almost nearly spherical in shape with crystallite sizes in the range 5.11-11.66 nm with some agglomeration. TEM images of PdS showed monodisperse nanocrystal with crystallite sizes ranging from 10.65-16.23 nm and the individual PdS nanocrystals are well separated without any agglomeration.

(Received July 15, 2016; September 16, 2016)

*Keywords:* Imidazolyl dithiocarbamate; NiS; PdS; nanoparticles; structural properties.

### 1. Introduction

Transition metal complexes have attracted attention for the synthesis of semiconductor nanocrystals [1-6]. At present, research into the synthesis of nanostructure materials has received considerable attention [7, 8] due to their very small sizes and large surface area that give them unique properties compared to the corresponding bulk materials [9-13]. Among semiconducting nanomaterials, metal sulfide nanocrystals have been extensively studied due to their importance in interpreting quantum size effects [14] and potential applications in many devices such as solar cells [15, 16], sensors [17], light-emitting diodes [18], fuel cells [19] and lithium-ion batteries [20]. Among all metal sulfide nanostructure materials, nickel sulfide has attracted attention due to their potential applications as catalysts and cathode material for rechargeable lithium battery, infrared detectors, hydro sulfurization catalysis, photoconductive material, solar storages among others [21-23]. Nickel sulfide have different stoichiometry and exist in different phases which make it more attractive and interesting but complicated to study [24]. The study of palladium based compound is interesting because of its potential application in catalysis [25-27], semiconducting electronic devices [28] and materials science [29]. Some PdS nanocrystals have been prepared using single source precursor's method [30, 31].

Several methods are being use to synthesise semiconductor nanoparticles but some often lead to the formation of aggregated nanoparticles which are caused by high surface energy and the restrictions of control over particle sizes [32-37]. Despite numerous efforts, it remains an ongoing challenge to get a reliable and reproducible facile methods for the synthesis of high quality nanocrystals. The use of single source precursor method thus remain one of the best method to synthesise high quality nanocrystals where shapes and sizes could be tune by varying reaction concentrations, time and temperature [38-42]. In this study, we report the use of imidazolyl

---

\*Corresponding author: pajibade@ufh.ac.za

dithiocarbamate complexes of Ni(II) and Pd(II) as single source precursors to synthesize NiS and PdS nanoparticles at 220 °C. The optical and structural properties of the resulting nanocrystals were studied with optical absorption and emission spectroscopy, powder X-ray diffraction (XRD), transmission electron microscopy (TEM), scanning electron microscopy (SEM) and energy dispersive X-ray spectroscopy (EDS).

## 2. Experimental

### 2.1. Materials and physical measurements

All chemicals and reagents were of analytical grade and used as obtained without further purification. The potassium salt of the ligand, imidazolyl dithiocarbamate were prepared by methods reported in the literature [43] and Pd(CH<sub>3</sub>CN)<sub>2</sub> was prepared by literature method [44]. A Perkin Elmer Lambda 25 UV-Vis spectrophotometer was employed to carry out optical measurements at room temperature. The photoluminescence of the nanoparticles were measured using Perkin Elmer LS 45 fluorimeter. Powder X-ray diffraction patterns were recorded on Bruker-D8 advance powder X-Ray diffractometer instrument operating at a voltage of 40 kV and a current of 30 mA with Cu K $\alpha$  radiation. The X-ray diffraction data were analysed using EVA (evaluation curve fitting) software. The phase identification was carried out with the help of standard JCPDS database. The transmission electron microscopy (TEM) images were obtained using a ZEISS Libra 120 electron microscope operated at 120 kV. The samples were prepared by placing a drop of a solution of the sample in toluene on a carbon coated copper grid (300 mesh, agar). Images were recorded on a mega view G2 camera using iTEM Olympus software. The scanning electron microscopy (SEM) images were obtained on a Joel, JSM-6390 LV apparatus, using an accelerating voltage between 15-20 kV at different magnifications. Energy dispersive spectra were processed using energy dispersive X-ray spectroscopy (EDS) attached to a Jeol, JSM-6390 LV SEM with Noran system Six software.

### 2.2 Synthesis of nickel(II) and palladium(II) imidazole dithiocarbamate complexes

The precursor complexes [bis(imidazolyl dithiocarbamato)M(II)], [M = Ni and Pd], were prepared as follows: 2.5 mmol of the respective metal salts: NiCl<sub>2</sub> or Pd(CH<sub>3</sub>CN)<sub>2</sub> was dissolved in 10 mL methanol and added to 10 mL methanol solution of imidazole dithiocarbamate (0.53 g, 5 mmol). Solid precipitates formed immediately and the mixture was stirred for about 3 hrs, filtered off and rinsed several times with distilled water and recrystallized with appropriate solvents.

### 2.3 Preparation of the NiS and PdS nanoparticles

0.40 g of the respective metal precursor was dissolved in 4 mL of TOP and injected into 3 g of hot hexadecylamine at 220 °C. A constant temperature was maintained for a period of 1 hr under the flow of nitrogen while stirring. The mixture was cooled to room temperature and excess methanol was added to precipitate the nanoparticles and remove excess HDA. The precipitates were separated by centrifugation and washed with methanol and the resulting solid precipitates of HDA capped NiS or PdS nanoparticles were dried at room temperature.

## 3. Results and discussion

### 3.1. Spectroscopic studies

The FTIR spectra of the imidazolyl dithiocarbamate ligand show distinct vibrational bands at 1003-1029 and 973-991 cm<sup>-1</sup> that can be assigned to  $\nu(\text{CS}_2)$  vibration of the dithiocarbamate moiety [45]. In the imidazolyl ligand, the  $\nu(\text{C-S})$  appear as two bands at 739 and 1188 cm<sup>-1</sup>. In the Ni(II) and Pd(II) complexes, the presence of only one strong absorption band suggests that the imidazolyl dithiocarbamate ligand is symmetrically bounded to the metal ions in a bidentate chelating modes [46]. The bands in the 1315-1425 cm<sup>-1</sup> region in the complexes with the thioureide  $\nu(\text{C=N})$  vibration is appreciably higher compared to what was observed in the ligand.

This indicates a significant increase in the partial double bond character of the dithiocarbamate C—N bond [47].

The composition of imidazolyl dithiocarbamate and the metal complexes were further checked by NMR spectroscopy. The compounds display well-resolved  $^1\text{H}$  and  $^{13}\text{C}$  NMR signals that integrate well to the corresponding hydrogen atoms in the compounds. A shift was observed in the  $\nu(\text{C-S}_2)$  spectra of the complexes compared to the free imidazolyl ligand confirming the bonding of the metal ion to the sulfur atom in M—S bond in the complexes [45]. The electronic spectrum of the imidazolyl dithiocarbamate show absorption band at 297 nm and 303 nm assigned to  $\pi \rightarrow \pi^*$  transition of the NCS of the dithiocarbamate moiety and  $n \rightarrow \pi^*$  on the sulfur atom. The electronic spectrum of the Ni(II) complex showed an intense ligand to metal charge transfer transitions at 337 nm and prominent d-d transition at 419 and 478 nm characteristic of Ni(II) complex in a square planar geometry. Pd(II) usually form square planar complexes with their electronic spectra dominated by charge transfer transitions. The electronic spectrum of the Pd(II) complex showed weak broad band at 460 nm that confirms the complex is in a square planar geometry.

### 3.2. Optical properties of the nanoparticles

The optical absorption spectra of the NiS and PdS nanoparticles are shown in Figure 1. The band edges of the synthesised NiS and PdS nanoparticles prepared from imidazole dithiocarbamate complexes were found to be 310 and 321 nm respectively. These band edges were used to determine the band gaps,  $E_g$  of the nanoparticles using the following equation [48]:

$$E_g = hc/\lambda$$

Where  $E_g$  = band gap,  $\lambda$  = cut off wavelength,  $h$  = Planks constant =  $6.626 \times 10^{-34}$  Joules sec,  $C$  = speed of light =  $3.0 \times 10^8$   $\text{ms}^{-1}$ . The band gaps of the synthesised NiS and PdS nanoparticles were calculated and found to be 4.04 and 3.90 eV respectively. This was found to be blue shifted compared to the bulk [49]. This shows that the prepared NiS nanoparticles have very small sizes and the increase in band gaps with decrease in particle size shows the quantum confinement effect [50]. Optical spectra for a range of nanocrystalline semiconductor show a blue shift in the absorption edge as the particle size decreases. This shift is ascribed to quantum size effect of the nanoparticles.

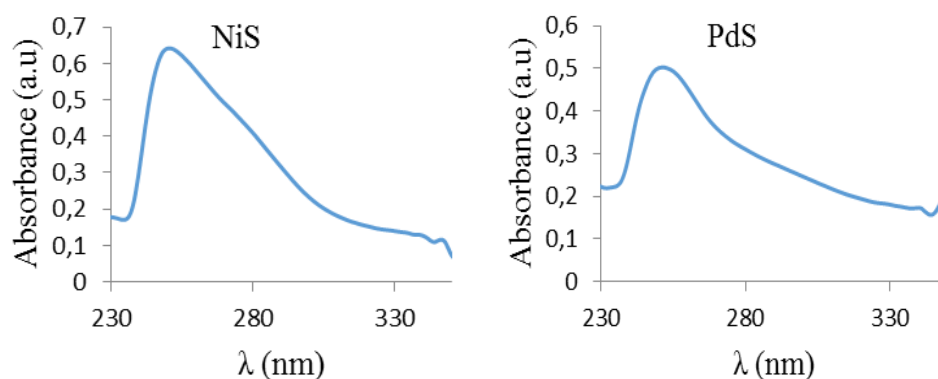


Fig. 1: Electronic spectra of NiS and PdS nanoparticles

Photoluminescence spectra of HDA-capped NiS and PdS nanoparticles were recorded at excitation wavelength of 711 nm and the resulting spectra are shown in Fig. 2. The spectra showed narrow emissions with emission maxima at 720 and 676 nm respectively. These PL peaks were found to be red shifted when compared to the optical absorption band edges [51]. Size distribution caused the broadening of the emission peaks as shown in Fig 2.

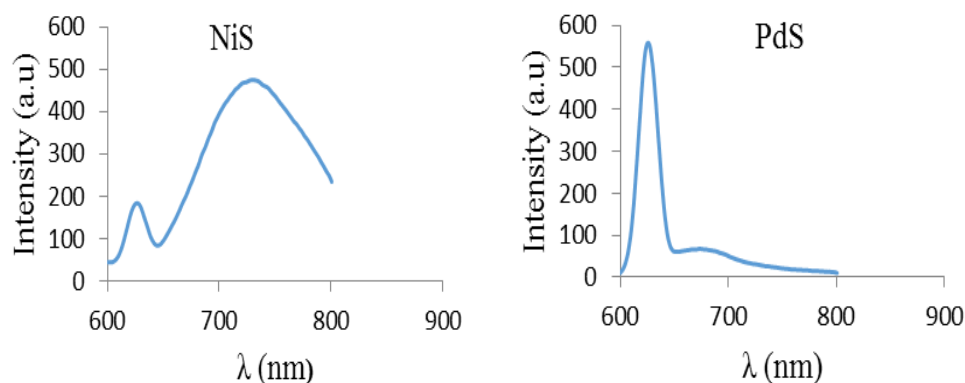


Fig 2: Photoluminescence spectra of NiS and PdS nanoparticles

### 3.3. X-ray diffraction studies of the nanoparticles

The XRD patterns of the NiS and PdS nanoparticles are presented in Fig 3. The crystalline phase of NiS was observed at  $2\theta$  values of 20, 21, 22, 23 and 26°, which corresponds to (211), (121), (220), (221) and (222) indices respectively. The XRD patterns can be indexed to the rhombohedral crystalline phase of nickel sulfide (JCPDS card no. 02-1280) [52]. Three peaks at  $2\theta$  values = 20.42, 21.48, and 22.98 degree corresponding to (221), (310), and (221) planes of PdS were observed. The XRD is indexed to the tetragonal PdS phase (JCPDS card no 78-0206). The broadness of the peaks is the indication of small particle size. The elongation of the XRD patterns is ascribed to the HDA capping agent used in the synthesis of the nanoparticles [53].

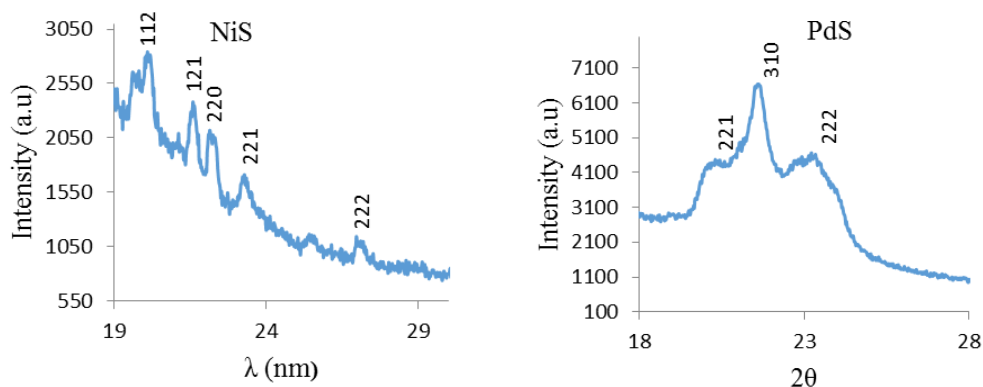


Fig. 3: XRD spectra of NiS and PdS nanoparticles 220 °C

### 3.4. The morphologies of the NiS and PdS nanoparticles

The morphology and microstructures of the NiS and PdS nanoparticles were characterized by TEM, SEM and EDS. The TEM image of NiS nanocrystals as shown in Figure 4(A), shows almost small spherically shaped nanoparticles with sizes in the range 5.11-11.66 nm and some of the particles aggregated to larger particles. The TEM image of PdS nanoparticles as presented in Figure 4(B) shows well aligned monodispersed spherically shaped nanoparticles that are well separated with almost uniform size distributions without aggregation. The particles size of the PdS nanoparticles are in the range 10.34-16.23 nm.

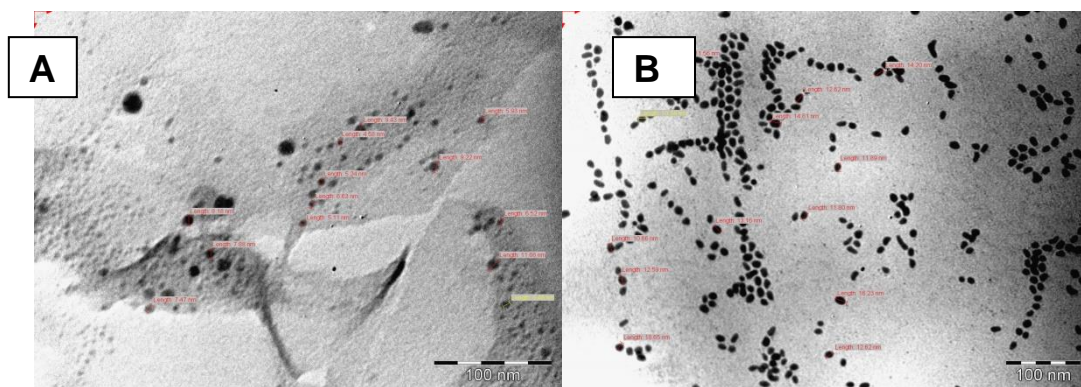


Fig. 4: TEM images of NiS (A) and PdS (B) nanoparticles

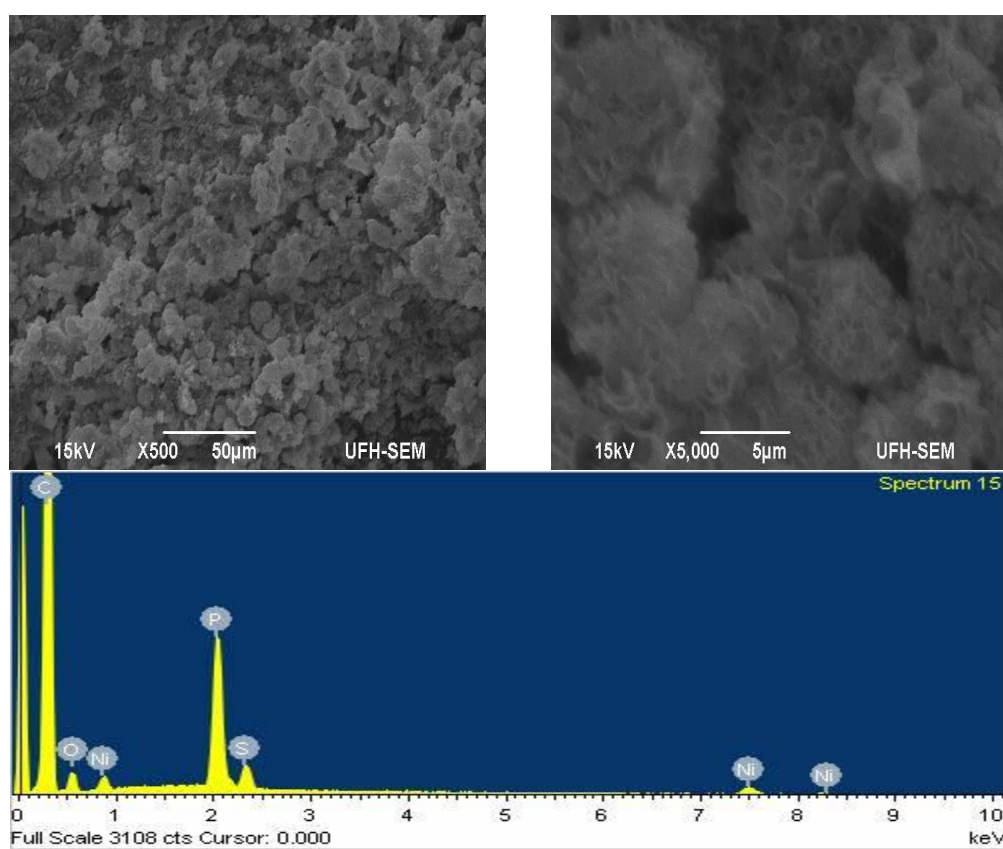


Fig. 5: SEM Images of NiS nanoparticles at low and high magnifications and EDS spectrum

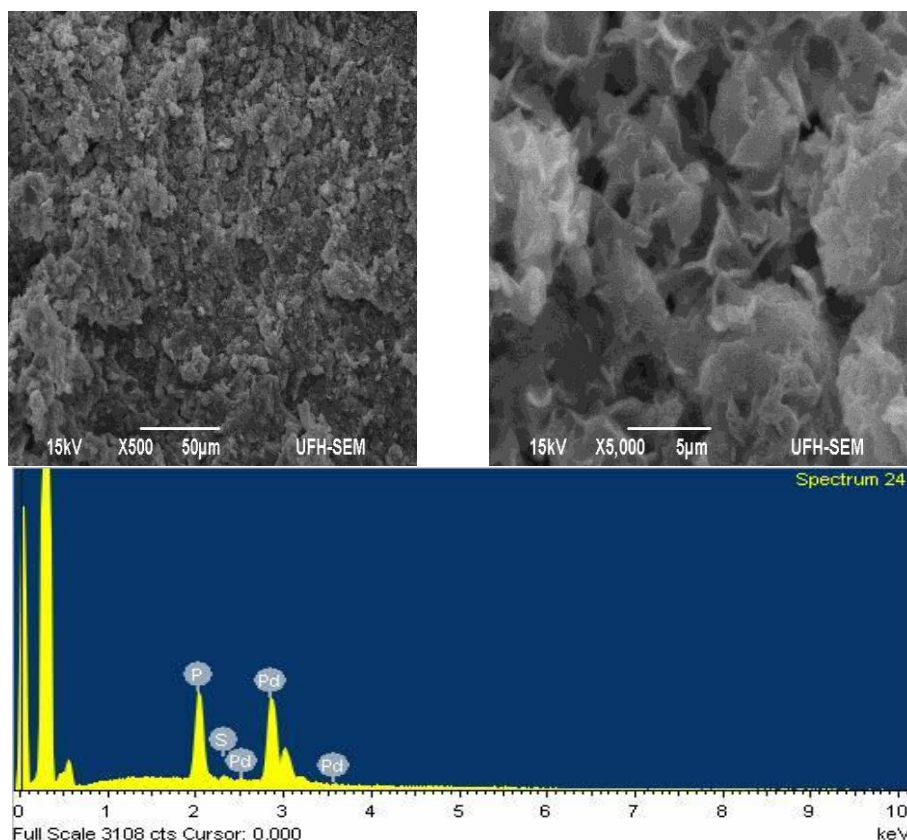


Fig. 6: SEM Images of PdS nanoparticles at low and high magnifications and EDS spectrum

The surface morphologies of the NiS and PdS nanocrystals were analysed by scanning electron microscopy (SEM). The SEM images at different magnifications are shown in Figures 5 and 6 for NiS and PdS nanoparticles respectively. The SEM images of NiS nanoparticles show that at low magnification, the morphology of the particles consist of small spherically shaped particles with some small pores in between them. At high magnification, the morphology are fine and smooth with fine structure that are closely packed together but the open pore spaces are more pronounced. The EDS spectrum confirmed the formation of NiS with the presence of Ni and S and other peaks such as C, O and P are from the trioctylphosphine and the hexadecylamine capping agent. The SEM images of PdS nanoparticles show slightly smooth/quirky morphology at low magnification. This morphology seems to be formed by irregular spheres. At high magnification, it looks like petals or micro platelets and the spaces between the particles are more visible. The EDS spectrum confirmed the formation of PdS with the presence of Pd and S peaks.

#### 4. Conclusions

In this study, we described the use of bis(imidazolyl dithiocarbamate) Ni(II) and Pd(II) complexes as single source precursor to synthesize NiS and PdS nanoparticles. Absorption spectra of the as-prepared NiS and PdS nanoparticles are blue shifted compared to bulk material indicating they are quantum confined due to their small crystallite sizes while the photoluminescence spectra show narrow emissions that are red-shifted. The XRD patterns of the NiS nanocrystals were indexed to hexagonal structure while the XRD of the PdS revealed the tetragonal crystalline phase. The TEM analysis indicate that the individual NiS nanoparticles are almost nearly spherical in shape with crystallite sizes of 5.11-11.66 nm with some agglomeration. TEM images of PdS nanocrystals revealed nanocrystals that are uniformly shaped without any agglomeration with average crystallite sizes of 10.34-16.23 nm.

## Acknowledgement

We gratefully acknowledge the financial support of Govan Mbeki Research and Development Centre, University of Fort Hare, SASOL South Africa and National Research Foundation/Sasol Inzalo Foundation for the award of innovation doctoral scholarship to AN.

## References

- [1] Z. Libor, Q. Zhang, *Mater. Chem. Phys.* **114**, 902 (2009).
- [2] S.L. Pal, U. Jana, P.K. Mana, G.P. Mohanta, R. Manavalan, *J. Appl. Pharm. Sci.* **1**, 228 (2011).
- [3] W. Brostow, M. Dutta, J.R. Souza, P. Rusek, A.M. Medeiros, E.N. Ito, *Expr. Polym. Lett.* **4**, 570 (2010).
- [4] O. Zhao, E.T. Samulski, *Polymer*, **47**, 663 (2006).
- [5] A. Anzlovar, Z.C. Orel, K. Kogej, M. Zigon, *J. Nanomet.* **1** (2012).
- [6] F. Yang, G.L. Nelson, *J. Appl. Sci.* **91**, 3844 (2004).
- [7] Banerjee. M.; Chongad. L.; Sharma. Res. J. Recent. Sci. **2**, 326 (2013).
- [8] W. Xu, Y. Wang, R. Xu, S. Liang, G. Zhang, D. Yin, *J. Mater. Sci.* **42**, 6942 (2007).
- [9] Y.G. Morozov. O.V. Belovsova, M.V. Kuznetsov, *Yug. Mater. Sci. Soc. Conf.* **56**, 231 (2009).
- [10] X. Wang, J. Zhuang, Q. Peng, Y. Li, *Nature Sci.* **437**, 121 (2005).
- [11] S. Wang, S. Yang, *Phys. Lett.*, **322**, 567 (2000).
- [12] W. Schmidt, *Appl. Organomet. Chem.* **15**, 331 (2001).
- [13] T.M. Ruhland, J.R.V. Lang, H.G. Alt, A.H.E. Muller, *Eur. J. Inorg. Chem.* 2146 (2013).
- [14] A. Monohar. K. Ramalingam. K. Karpagavel. *J. Chem. Tech. Res.* **4**(4), 1383 (2012).
- [15] F. Atay. S. Kose. V. Bilgin. I. Akyuz, *Turk. J. Phys.* **27**, 285 (2003).
- [16] R. Wang. H. Wang. H. J. S. Feng, *Int. J. Electrochem. Sci.* **8**, 6068 (2013).
- [17] D. Baogen. Y. XiaoZhen, Z. XiongFeri. H. S. Ling. S. WenHua, *Sci China Ser-B-Chem* **1** (2008).
- [18] J. Cookson, *Platinum Metals Rev.*, **56**, 83 (2012).
- [19] D. Astruc, *Inorg. Chem.*, **46**, 1884 (2007).
- [20] A. T. Bell, *Science*, **299**, 1688 (2003).
- [21] N. Semagina, A. Renken and L. Kiwi-Minsker, *J. Phys. Chem. C*, **111**, 13933 (2007).
- [22] Z. Hou, N. Theyssen, A. Brinkmann and W. Leitner, *Angew. Chem. Int. Ed.*, **44**, 1346 (2005).
- [23] R. Narayanan and M. A. El-Sayed, *J. Catal.*, **234**, 348 (2005).
- [24] S. Cheong, J. D. Watt and R. D. Tilley, *Nanoscale*, **10**, 2045 (2010).
- [25] A. Mashkina and L. Sakhaltueva, *Kinet. Catal.*, **43**, 107 (2002).
- [26] P. Raybaud, J. Hafner, G. Kresse and H. Toulhoat, *J. Phys. Condens. Matter*, **9**, 11107 (1997).
- [27] M.A. Ehsan, H.N. Ming, V. Mckee, T.A.N. Peiris, V. Wijayantha-Kahagala-Gamage, Z. Arifin, M. Mazhar, *New J. Chem.* **34**, 4083 (2014).
- [28] I. Ferrer, P. Di'az-Chao, A. Pascual and C. Sa'nchez, *Thin Solid Films* **515**, 5783 (2007).
- [29] K. E. K. Yamamoto, K. Endo, Y. Takaya and E. Kaneda, *Japanese Patent*, **62**(226), 155 Mitsubishi Paper Mills Ltd., (1987).
- [30] J. Cheon, D.S. Talaga, J.I. Zink, *Chem. Mater.* **9**, 1208 (1997).
- [31] M.A. Malik, P. O'Brien, N. Revaprasadu, *J. Mater. Chem.* **12**, 92 (2002).
- [32] W. Wang, Z. Liu, C. Zheng, C. Xu, Y. Liu and G. Wang, *Mater. Lett.* 2755 (2003).
- [33] K. Ramasamy, M. A. Malik, M. Helliwell, J. Raftery, P. O'Brien, *Chem. Mater.* **23**, 1471 (2011).
- [34] M. A. Malik, M. Afzaal and P. O'Brien, *Chem. Rev.*, **110**, 4417 (2010).
- [35] N. Ghows and M. H. Entezari, *Ultrason. Sonochem.*, **18**, 269 (2011).
- [36] N. Srinivasan, S. Thirumaran and S. Ciattini, *J. Mol. Struct.*, **1026**, 102 (2012)
- [37] J. Park, J. Joo, S. G. Kwon, Y. Jang and T. Hyeon, *Angew. Chem., Int. Ed.*, **46**, 4630 (2007).
- [38] N.L. Pickett, P. O'Brien, *The Chem. Rec.* **1**, 467 (2001).
- [39] C.J. Barrelet, Y. Wu, D.C. Bell, C.M. Lieber, *J. Am. Chem. Soc.* **125**, 11498 (2003).

- [40] I.J.-L. Plante, T.W. Zeid, P. Yang, T. Mokari, *J. Mater. Chem.* **20**, 6612 (2010).
- [41] V.A.V. Schmachtenberg, G. Tontini, J.A. Koch, G.D.L. Semione, V. Drago, *J. Phys. Chem. Sol.* **87**, 253 (2015).
- [42] J.Z. Mbese, P.A. Ajibade, *J. Sulf. Chem.* **35**, 438 (2014).
- [43] N.L. Botha, P. A. Ajibade, *Mater. Sci. Semicond. Process.* **43**, 149 (2016).
- [44] G.K. Anderson, M. Lin, *Inorg. Synth.* **28**, 60 (1990).
- [45] P.A. Ajibade, B.C. Ejelonu, *Spect. Chim. Acta Mol. Biomol. Spectr.* **113**, (9) 4044 (2013).
- [46] K.S. Siddiqi, N. Nishat, *Synth. React. Inorg. Met-Org. Nano-Met. Chem.* **30**, 1505 (2000).
- [47] S.A.A. Nani, K.S. Siddiqi, 34 92004) 1583-1593.
- [48] M.M.Abdo, G. Elham, S. Nayereh, W.M.Y. Mahmood, S. Elias, *Polymers*, **6**, 2435 (2014)
- [49] M. Banerjee, L. Chongad, A. Sharma, *Res. J. Recent. Sci.* **2**, 326 (2013).
- [50] N. Sahiner, K. Sel, K. Meral, Y. Onganer, S. Butun, O. Ozay, C. Silan, *Col. Surf. A: Physiochem. Eng. Aspects.* **389**, 6 (2011).
- [51] M.A. Languna, V. Paillard, B. Kohn, M. Ehbrecht, F Huisken, G. Ledoux, R, Papoular, H. Hofmeister, *J. Lumin.* **80**, 223 (1999).
- [52] C. Sim, M. Ma, J. Yang, Y. Zhang, P. Chen, W. Huang, X. Dong, *Scient. Reports*, **4**, 1 (2014).
- [53] H.R. Pouredal, R. Momenzadeh, *Bulg. Chem. Commun.* **11**, 59 (2015).
- [54] Z. Yang, B.A. Smetana, C.M. Sorensen, K.J. Klabunde, *Inorg. Chem.* **46**, 2427 (2007).